Circuit Simulations for the RMF$_O$/FRC Antenna System

Jonathan Sapan
Princeton Department of Electrical Engineering and
Princeton Plasma Physics Laboratory
May 2002

Abstract

Resonance and impedance matching conditions for an RF antenna system were analyzed using SIMmetrix, a SPICE-based circuit simulator. The antenna, being designed for a plasma heating experiment, consists of two parallel inductors (antenna arms) with variable series and parallel capacitors added for tuning and impedance matching. The plasma response is considered purely resistive, with a typical value of 100mΩ. The analyses produced operating curves defined by pairs of series/parallel capacitance values that would allow antenna operation in the frequency range 5 to 15 MHz while minimizing reflected power. Current along operating curves was found to be constant for specified transmission lines and antenna inductance. Antenna-arm current was found to be proportional to the inverse-square root of the resistive plasma impedance. Because of the low inductance of the antenna, transmission lines of typical length 1-3 m were found useful for impedance matching in the lower range of the frequencies. The effects of realistic (±5%) asymmetries in the two parallel antenna-arm circuits were examined and found to be alter antenna currents and phases by < 3% and 3° respectively. Worst-case circuit asymmetries and parameter choices (i.e., changing antenna inductance from 85nH to 340nH) still allowed for 150A currents through the antenna-arms (inductors), corresponding to a 5G peak magnetic field strength, over a 6-10 MHz frequency range, with the voltage on the parallel capacitor remaining below ~12kV and inductor voltage remaining below ~6kV.

I. Introduction

The RMF_O/FRC apparatus is an experimental plasma device at the Princeton Plasma Physics Laboratory being used to investigate fusion physics in an innovative confinement configuration. Plasma confinement will be achieved by means of a radio-frequency (RF) antenna system, which will be used to generate currents in target plasma and also to heat the plasma. In preparation for driving the antenna system with voltages in the range of several kilovolts, an antenna circuit was designed and a commercial numerical model was used (SIMmetrix, a SPICE based simulator, by Newburry Technology, Berkshire, UK) to predict circuit performance over a broad range of possible circuit parameters.

In brief, an antenna circuit consists of an inductor (the antenna proper) and two capacitors, one in series (C_s) and one in parallel with the antenna (C_p). Sets of values for series and parallel capacitors in the tuning circuit necessary to yield the desired antenna current were found. Operation regimes which could damage circuit components (e.g. high-power RF amplifiers, voltage-limited capacitors) were identified. The effects of varying circuit parameters were explored.

The RMF_O/FRC apparatus has two such antenna circuits. Each antenna circuit contains two inductors in parallel with each other (termed "antenna arms"; see circuit diagram, Figure 1). As installed, each antenna arm has an inductance of 85nH. The two pairs of antennae are oriented orthogonally to each other, resulting in negligible mutual inductance.

RF power should be coupled efficiently to plasmas. Optimal power transfer corresponds to minimal power reflected from the antenna circuits back to their respective power sources. These goals are equivalent to matching the RF power source impedance (50Ω) with the impedance of the load (the antenna circuit). Since components such as amplifiers and power sources are intolerant to high reflected power, impedance matching is particularly important. Therefore, the operation of the antennae is constrained by the desire to maintain impedance matching. With this is mind, it is necessary to determine circuit parameters (in this case, pairs of variable capacitance values, (C_s, Cp) for a given set of other fixed parameters) which will satisfy the constraint of impedance matching as well as other physical constraints (voltage/power limitations on capacitors and upper and lower limits on capacitances) and supply the maximum desired RF magnetic field strength (5G, equivalent to 150A peak circulating currents in each antenna arm or 300A total in each parallel antenna arm pair).

To determine circuit parameters for desired operation, SIMetrix, a SPICE-based circuit-simulator, was used. Since transmission lines cannot be accurately represented by shorts when transmitting high frequency signals, the connections between the tuning elements (capacitors) and the antenna arms, which, in the physical apparatus, will be comparatively long compared to any other connections (~2.4m long), were simulated using SIMetrix's built-in model for lossless transmission lines. A primary goal of the simulations was to generate pairs of capacitance values (C_s, C_p) that would allow antenna operation in the 5-15 MHz frequency range. Simulations were run for a number of scenarios involving changes and/or asymmetries (between the two antenna arms in a single antenna circuit) in circuit component values and effects upon circuit tuning (capacitor values) necessary to achieve desired antenna currents and impedance matching. Scenarios included increased antenna inductance (which might be effected by the construction of two-turn antenna arms), asymmetry in

antenna resistances and varying transmission line delays (both symmetrically and asymmetrically). Antenna resistance consists of two parts: the resistance of the copper antenna itself and an apparent resistance introduced by the plasma.

To determine operating points (OP) corresponding to matched impedances (antenna circuit impedance of 50Ω to match 50Ω source impedance), the antenna circuit was placed in series with a voltage source and a 50Ω resistor (the most elementary way of modeling a 50Ω source impedance). For a 100V source, the magnitude of the current through the circuit should be equal to 1A if the impedances are matched (the circuit can be seen as two 50Ω impedance blocks in series; $\frac{100V}{(2 * 50\Omega)} = 1A$).

The capacitance values were adjusted such that the circuit current at resonance equaled 1A. For a given set of fixed circuit parameters (antenna arm resistance, antenna arm inductance, and transmission line delay), pairs of series and parallel capacitance values yielding 1A at resonance were found. The plot of parallel capacitance vs. series capacitance for a given set of parameters will be called an "operating curve" (OC) hereafter. While the current for each point on an operating curve is 1A, the resonant frequency differs at each point.

Figure 1 shows the SIMmetrix schematic of the circuit simulated along with example plots of circuit current, parallel capacitor voltage, voltage drop across the transmission lines, inductor voltage, and inductor current (circuit parameters given in caption).

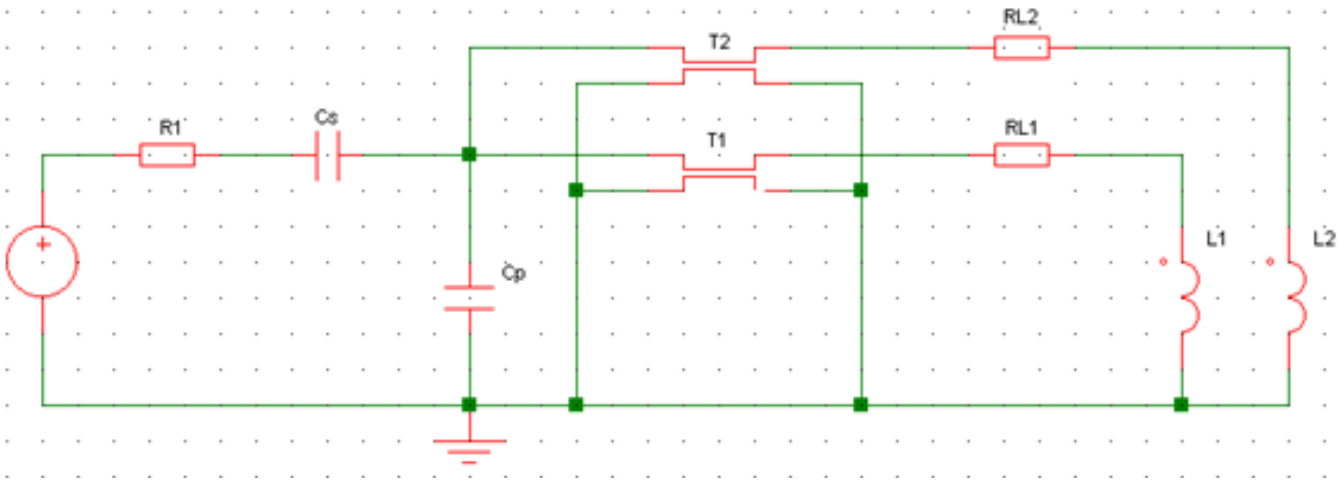

Figure 1a

Figure 1b

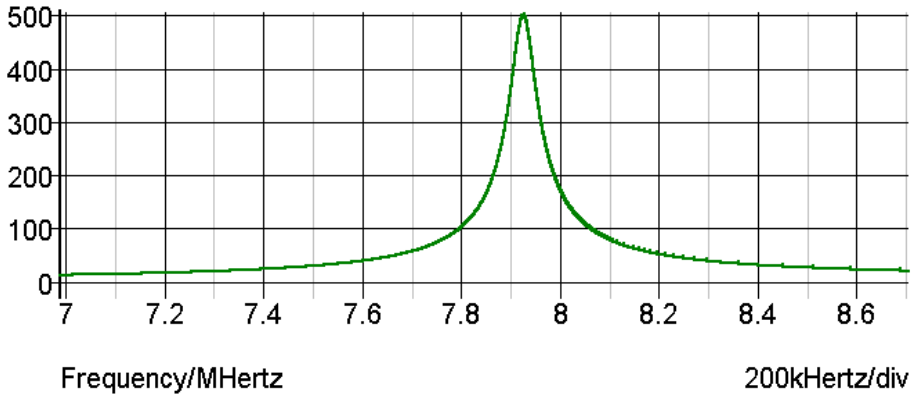

Figure 1c

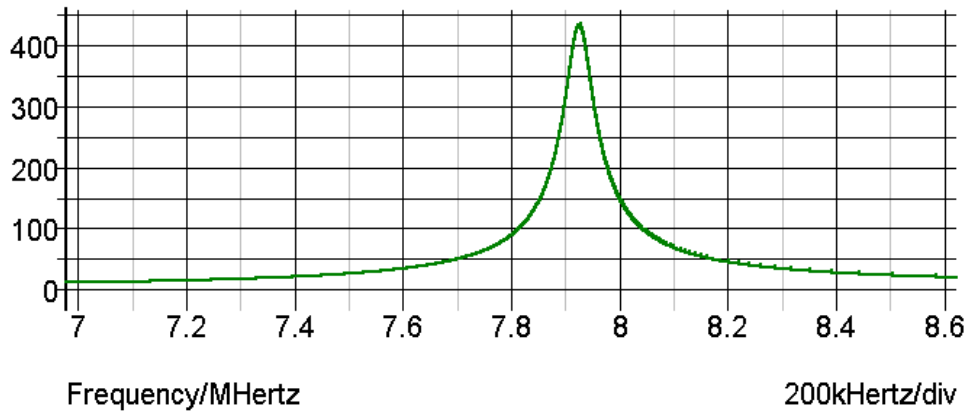

Figure 1d

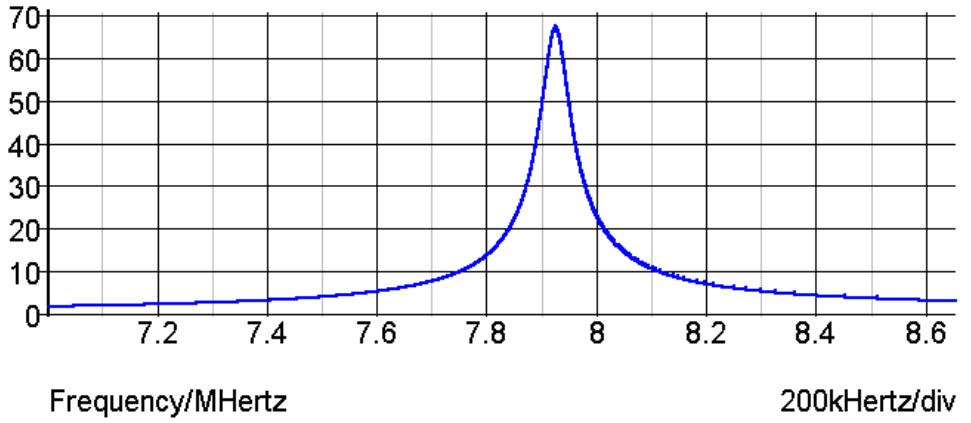

Figure 1e

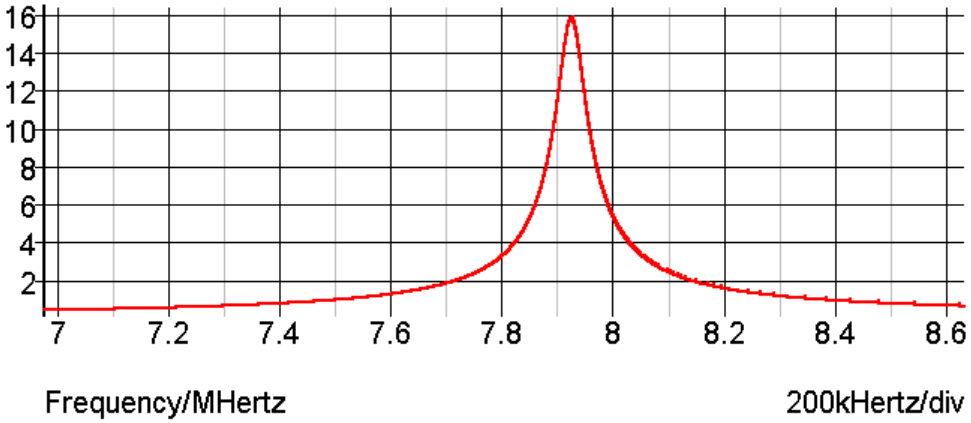

Figure 1f

Figure 1. [**a**] Circuit diagram from SIMetrix. [**b**] Plot of current in leftmost pin of C_s (I_{Cs}) in Amps. [**c**] Plot of parallel capacitor voltage (V_{Cp}) in Volts. [**d**] Plot of voltage drop across transmission lines in Volts. [**e**] Plot of inductor voltage (V_L) in Volts. [**f**] Plot of inductor current (I_L) in Amps. Circuit parameters for plots shown: R_1 = 50Ω, C_s = 40pF, Cp = 950pF, T_{d1} = T_{d2} = 12ns, R_{L1}=R_{L2} = 100mΩ, L_1 = L_2 = 85nH.

II. Operating Curves: Symmetric Variables

1. Theoretical Expectations

An intuitive sense of the performance of the antenna circuit can be gained by considering the circuit as a simple driven RLC circuit, neglecting the transmission line. In this model, resonant frequency should vary linearly with the inverse-square-root of the parallel capacitance (for a fixed inductance). An inductor and capacitor in parallel function as a reactive current divider. At low frequencies, most of the current will flow through the inductor and at high frequencies most of the current will flow through the capacitor. At resonance, the magnitudes of the capacitor and inductor impedances are equal and, consequently, so are the currents (though the currents will be 180º out of phase). The circuit quality, $Q = \frac{\omega_0 L}{R}$, will increase linearly with resonant frequency and decrease linearly with circuit resistance (the lumped resistance of the antenna inductance). The bandwidth (BW), defined as the width of the frequency band between the points where the curve value drops to one half its value at resonance on either side the resonance point, remains constant with frequency and is determined by L and R; the bandwidth is $\frac{1}{2\pi}\frac{R}{L}$ in Hertz[1].

The antenna circuit can be viewed as a capacitor in series with a reactive current divider (where the branches are: 1. the parallel capacitor and 2. the antenna inductance taken together with its resistance and the transmission line). The transmission line, in addition to introducing a propagation delay in the circuit, has the effect of adding additional inductance and capacitance to the circuit, proportional to its length. RG-214 cable adds 101 pF/m and approximately 253 nH/m, neglecting series resistance and shunt conductance. As discussed below, inductor currents are constant along an OC and depend only upon the series resistance of the inductor (in the case of asymmetric circuits, as in Section III, the *sum* of the two inductor currents will be constant). While one would expect an increase in inductor current with an increase in parallel capacitance (due to the decreasing impedance of a capacitor with increasing capacitance), raising the capacitance also *lowers* the resonant frequency, thus raising the parallel capacitor's impedance. The lowered resonant frequency also balances the capacitor's rising impedance against the inductor's falling impedance, resulting in constant inductor currents along the operating curves.

B. Antenna Inductance and Transmission Line Delay

Given any set of fixed, symmetrical parameters (i.e., transmission line delay, inductance and inductor resistance in one antenna arm equal to the corresponding value in the other antenna arm), operating curves follow straight, approximately parallel lines (see Fig. 2). For a fixed transmission line delay, curves for L=85nH lie only slightly above those for L=340nH, though there is a significant upward shift in resonant frequency between 340nH and 85nH. For a fixed inductance, *increasing* transmission line delay will *decrease* the offset of the operating curve (the effects of transmission line

---

[1] This follows from an alternate but equivalent definition of the circuit quality, $Q = \frac{f_0}{\Delta f}$ where Δf is the bandwidth.

delay are marked compared to the effects of varying inductance; see Figure 2), that is, shift the curve to a higher parallel capacitance at a fixed series capacitance and vice versa. For any point (C_s, C_p) on an operating curve for a symmetrical circuit (with the inductor resistances equal to 100mΩ), the current will be constant at 15.8A in each antenna arm.

Resonant frequency, parallel capacitor voltages and inductor voltages along a given operating curve are accurately described by power-law relationships (see Figures 3-5). It is interesting to note that the curves in Figures 3-5 appear to approach the form $k(C_s^{-1/2})$, where k is a constant, with decreasing transmission line delay and decreasing inductance. This makes intuitive sense when one considers that, were the antenna circuit to be to be modeled as a simple RLC circuit (see Section IIA above) with only a series a capacitor and antenna arm, the resonant frequency would indeed scale linearly with $C^{1/2}$; the presence of additional capacitance and inductance from the parallel capacitor and transmission lines would account for the deviation. As above, the plots more closely resemble an inverse square-root relationship when there is less fixed capacitance and inductance from the transmission line (lower transmission line delay) and when the antenna arm inductance is larger in proportion to the total circuit inductance (larger antenna arm inductance). In plots of voltage across the parallel capacitor (V_p) versus series capacitance (C_s) (Figure 4), curve fits have roughly equal exponents but higher initial values when the inductance is equal to 85nH, with the percentage offset decreasing for curve-pairs with higher transmission line delays. The height of the capacitor voltage curves on the plot (Figure 4) increases with increasing transmission line delay and increasing inductance. Ignoring the transmission line, higher inductances should result in more current flowing through C_p and thus a higher voltage across it. Transmission line delay can be said to result in a smaller voltage drop across the line and antenna arm, resulting in a higher I_{Cp} and thus V_{Cp}. Taking the maximum capacitor voltage plotted and scaling the input voltage such that the inductor currents = 150A (a stated goal) indicates that the voltage across the capacitor will not exceed ~9kV for any of the operating curves plotted (Figure 2).

Plots of inductor voltage (Figure 5) are similar to those for capacitor voltage, though curve height decreases with increasing transmission line delay rather increasing. If increasing transmission line delay results in a larger voltage drop across the transmission line, V_L can be expected to decrease with increasing transmission line delay. Given a fixed transmission line delay and antenna current, increasing L will result in increasing V_L (since $V = L\frac{di}{dt}$). Curves for a fixed transmission line delay have approximately equal exponents and, in each case, the initial values when the inductance are equal to 340nH are approximately 3.3 times the initial values for 85nH, suggesting a nearly linear dependence upon L. The deviation from linearity can be explained by the presence of additional inductance due to the transmission line (i.e., moving from L=85nH to L=340nH approximately represents a 330% increase in total circuit inductance as opposed to a 400% increase, which would be the case were the antenna arms the sole inductances in the circuit). Additionally, the three curves plotted for L=85nH are clustered in close vertical proximity (the lowest curve is initially separated by ~35V from the highest), with the height of the curves increasing with decreasing transmission line delay. Plots for L=340nH are also clustered together (though not as tightly; the initial separation is ~135V between the curve for 10ns and the curve for 20ns) and are separated by a large gap from the curves for L=85nH (~1.2kV initially). Scaling the highest plotted inductor voltage suggests that the inductor voltage will not exceed 5kV in

symmetrical circuit configurations with the antenna resistances equal to 100mΩ and inductances of 340nH. In 85nH circuits, inductor voltage will not exceed 1.5kV.

No operating curve corresponding to T_d=3ns, L=85nH was plotted. A circuit modeled with these parameters cannot be operated at resonance subject to impedance matching constraints within the desired frequency range (5-15 MHz) without a lower C_s (or higher C_p) than possible with the present components.

C. Antenna Resistance

With transmission line delay fixed at 12ns and antenna arm inductance at 85nH, an attempt was made to find operating curves for R_L equal to 10mΩ, 100mΩ (curves for this value are discussed in section A above and can be found plotted in Figure 2a), and 1Ω.

When R_L = .01Ω, the range of the operating curve is exceedingly narrow and can be approximated by a single operating point. At C_s = 15pF, and C_p = 1200pF, the resonant frequency is 7.26MHz, the V_P and V_L are 1.47kV and 194V, respectively, and the antenna arms currents are 50A. Operation at higher or lower frequencies would require a lower series capacitance or a higher parallel capacitance than possible with the present components.

The operating curve plotted for R_L = 1Ω has a shallower slope than the curve for 0.1Ω (m ≈ 11 vs. m ≈ 31), which is not surprising given the greater resistance (the increased impedance of the antenna arm inductance and resistance is balanced by the impedance of the capacitor, which depends inversely upon the capacitance). However, the relationship between antenna current and antenna arm resistance *is not* linear; the current follows the inverse-square root of the antenna arm resistance. Between the simulations discussed in this section and those in Section III, the relationship between total antenna current (I_{L1}+I_{L2}) is related to total antenna arm resistance (R_{L1}+R_{L2}) by the following equation: $I_{total} = \frac{14.139}{\sqrt{R_{total}}}$; R=1, $\chi^2 = .0031105$.

D. Circuit Quality (Q)

Since $Q = \frac{\omega_0 L}{R} = \frac{f_0}{\Delta f}$, the circuit quality will depend upon the bandwidth and the resonant frequency. The bandwidth will remain constant for fixed values for antenna inductance, antenna resistance, and transmission line delay (this can be seen by solving for the bandwidth in the above expression). The bandwidth was found as a function of transmission line delay for 85nH and 340nH circuits. The bandwidth was also found for 85nH circuits with 12ns delay times as a function of antenna resistance.

Plots of bandwidth vs. transmission line delay (Figure 10) obey power relationships, with plots for 85nH circuits steeper than those for 340nH circuits. This can be explained by the fact that the inductance added by increased transmission line delay is greater in proportion to the fixed inductance of the antenna in 85nH circuits. Plots of bandwidth vs. antenna resistance (Figure 11) display an approximately linear scaling with the inverse resistance, as would be expected from the equation.

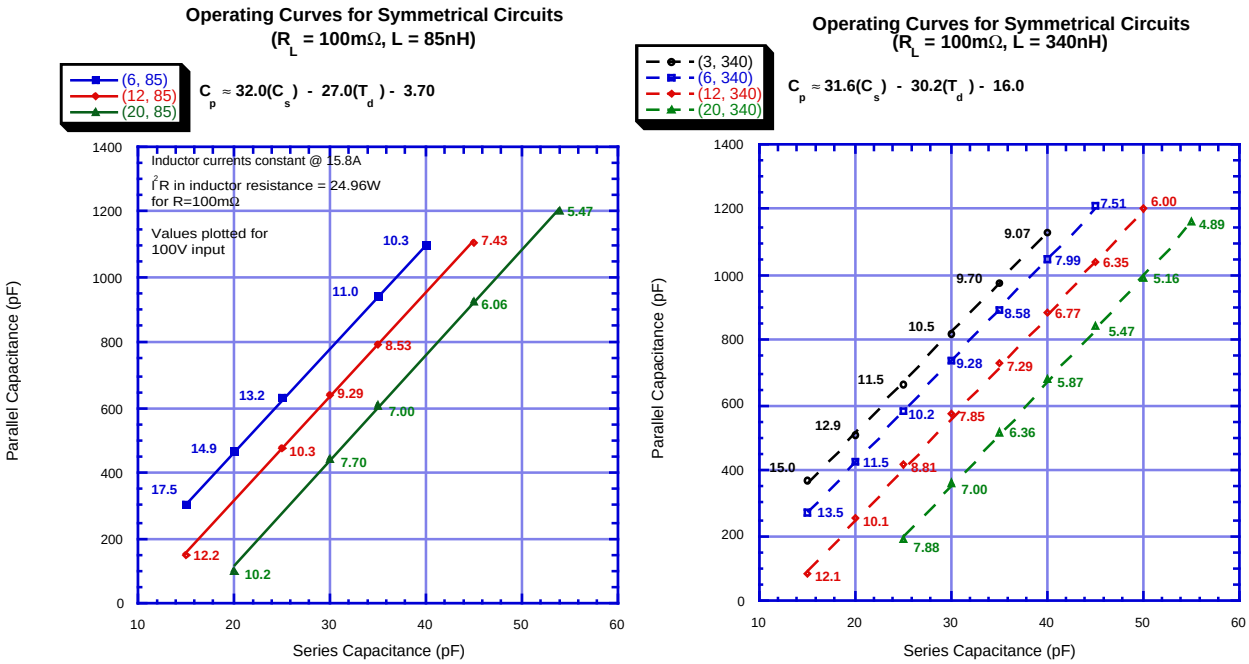

Figure 2. Operating curves for symmetrical circuits (delays, inductances, and resistances equal). Curves are denoted as (T_d, L), where T_d is the transmission line delays in ns and L is the antenna arm inductances in nH. Curves consist of pairs of capacitance values (series and parallel) that yield 1A of current in the circuit (which, as discussed, indicates impedance matching with the source impedance) given a $100V_{AC}$ input for the specified delay and inductance values. Curves of constant transmission line delay are the same color and have identical marker shapes; curves for 85nH are solid and those for 340nH are dashed. Resonant frequencies along each operating curve are noted for reference (see Figure 3 for complete plots).

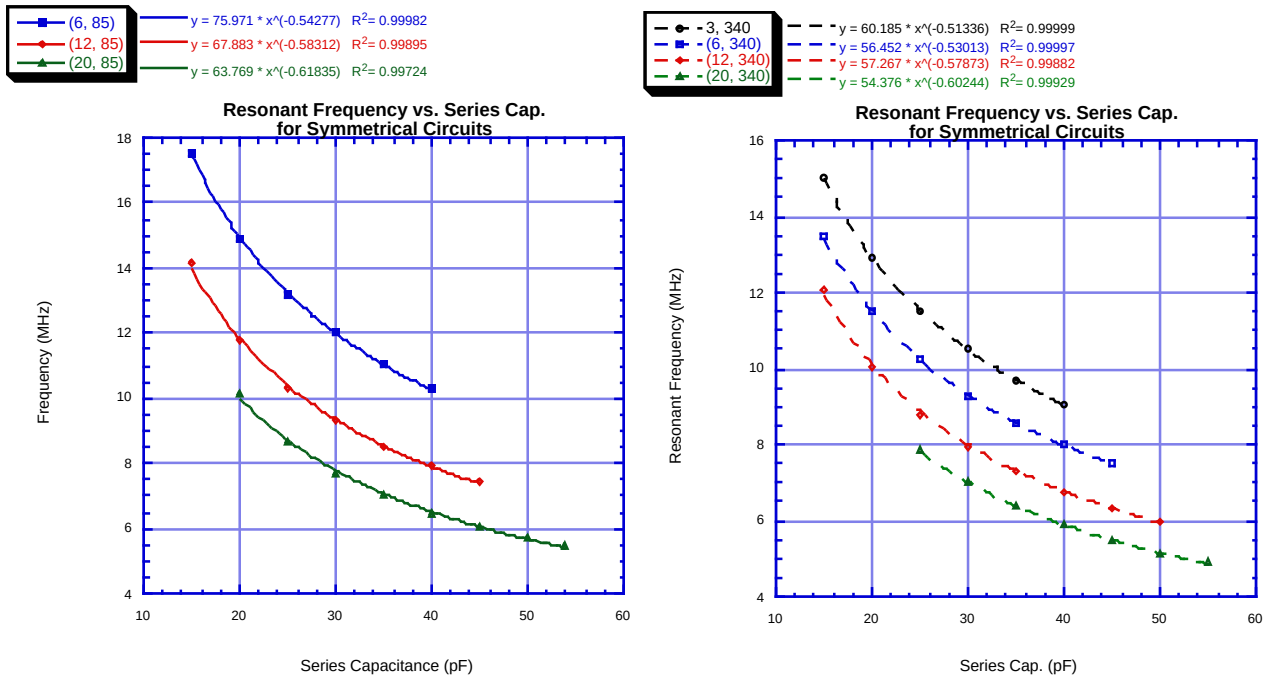

Figure 3. For a set of (C_s,C_p)parameters as specified in Figure 2, sets of resonant frequencies corresponding to each of the points along the operating curves in Figure 2 are plotted as a function of the series capacitance at the given point. Curves of constant transmission line delay are the same color and have identical marker shapes; curves for 85nH are solid and those for 340nH are dashed.

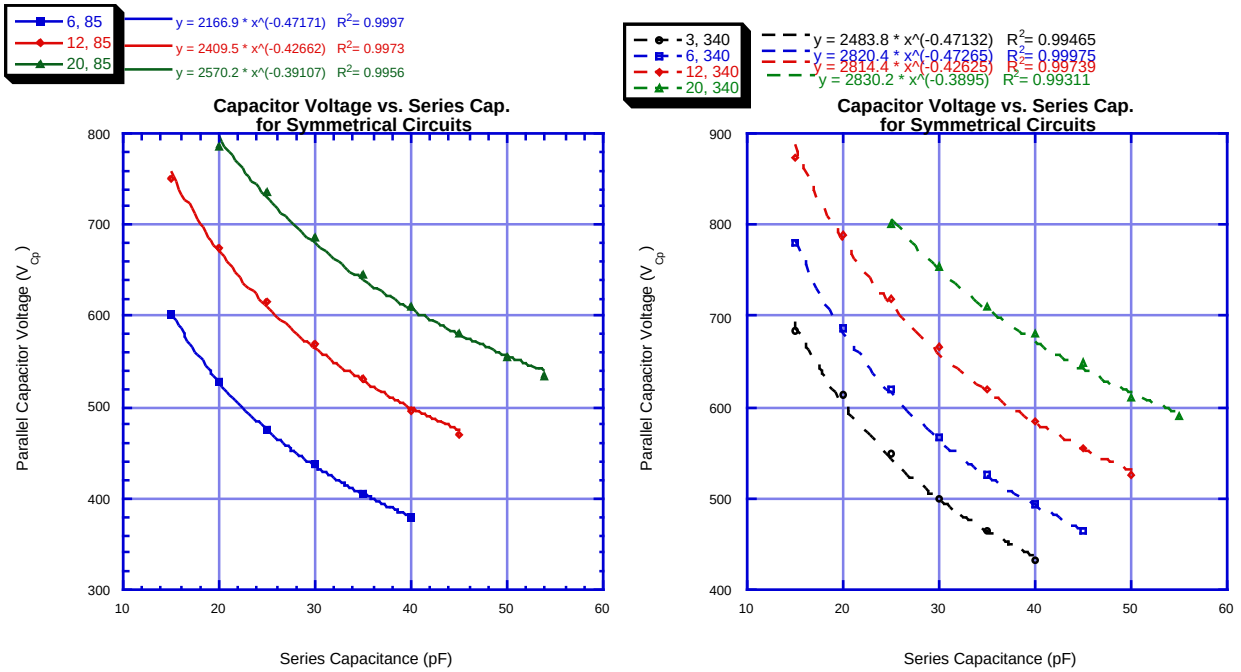

Figure 4. For a set of (C_s,C_p) parameters as specified in Figure 2, sets of voltages across the parallel capacitor corresponding to each of the points along the operating curves in Figure 2 are plotted as a function of the series capacitance at the given point. Curves of constant transmission line delay are the same color and have identical marker shapes; curves for 85nH are solid and those for 340nH are dashed. As above, values are plotted for 100V_{AC} input. The voltage will scale linearly with the current.

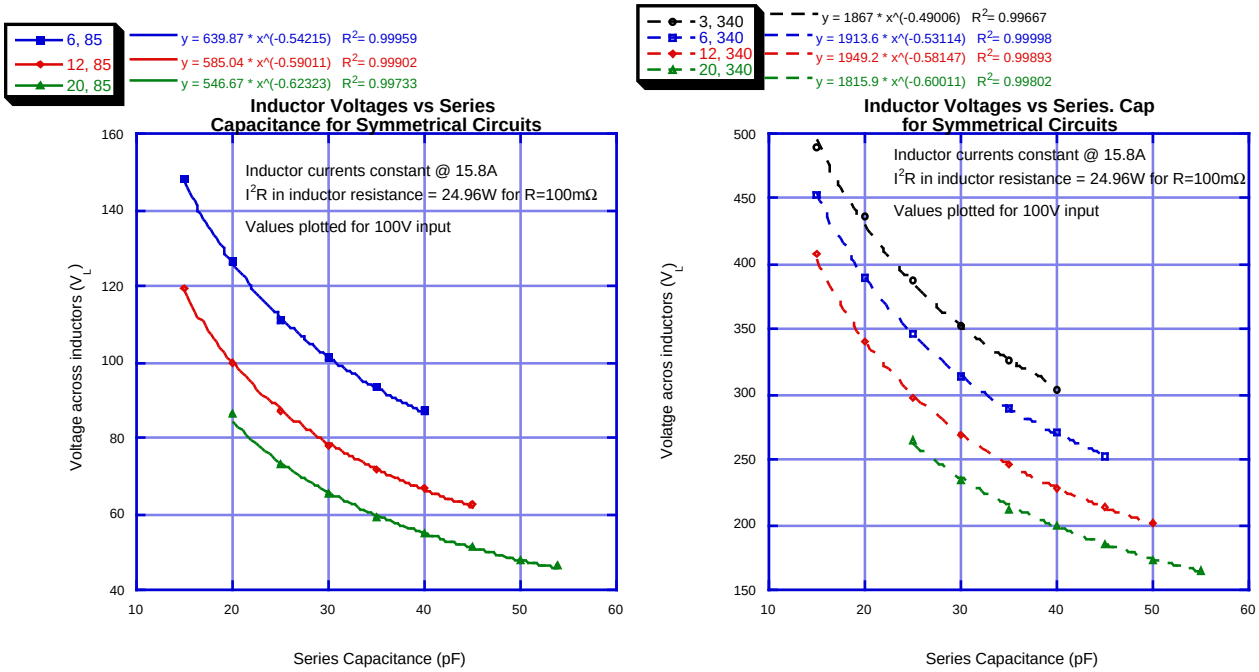

Figure 5. For a set of (C_s, Cp) parameters as specified in Figure 2, sets of voltages across the inductors corresponding to points along the operating curves in Figure 2 are plotted as a function of the series capacitance at the given point. Curves of constant transmission line delay are the same color and have identical marker shapes; curves for 85nH are solid and those for 340nH are dashed. As above, values are plotted for a 100V_{AC} input.

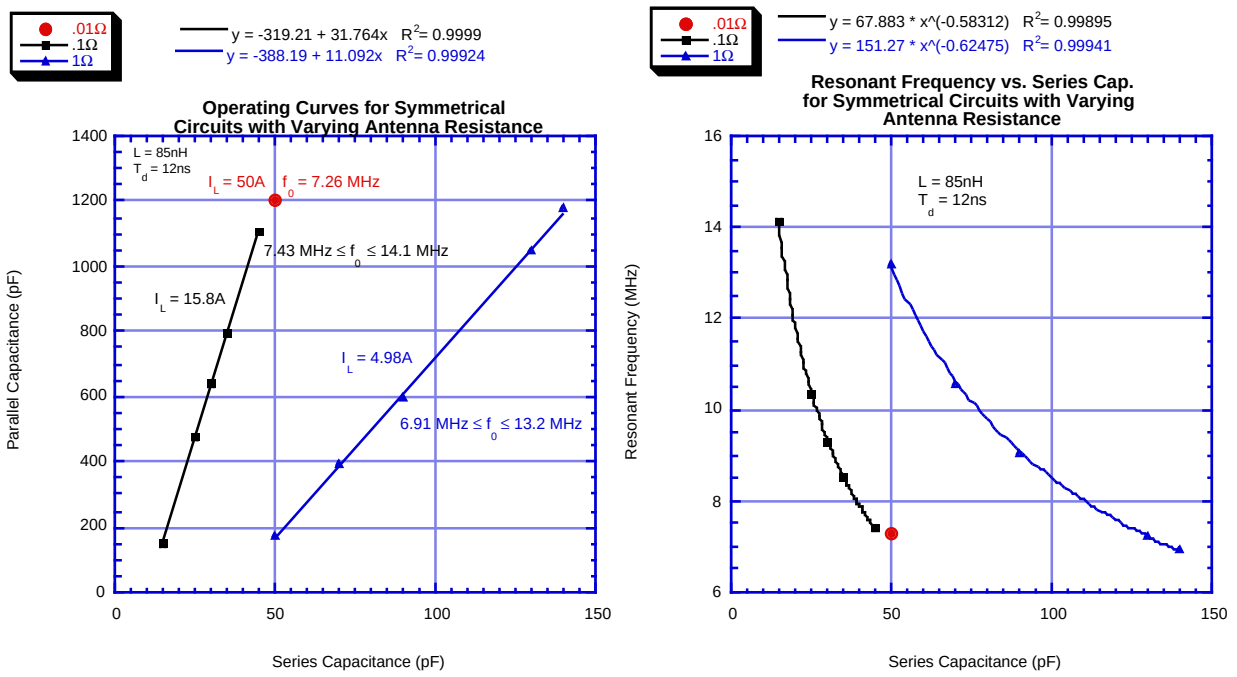

Figures 6 and 7. Operating curves (Figure 6) and plots of resonant frequency vs. series capacitance (Figure 7) for R_L between .01Ω and 1Ω. L = 85nH for all curves and T_d = 12ns. Compare with Figures 2 and 3.

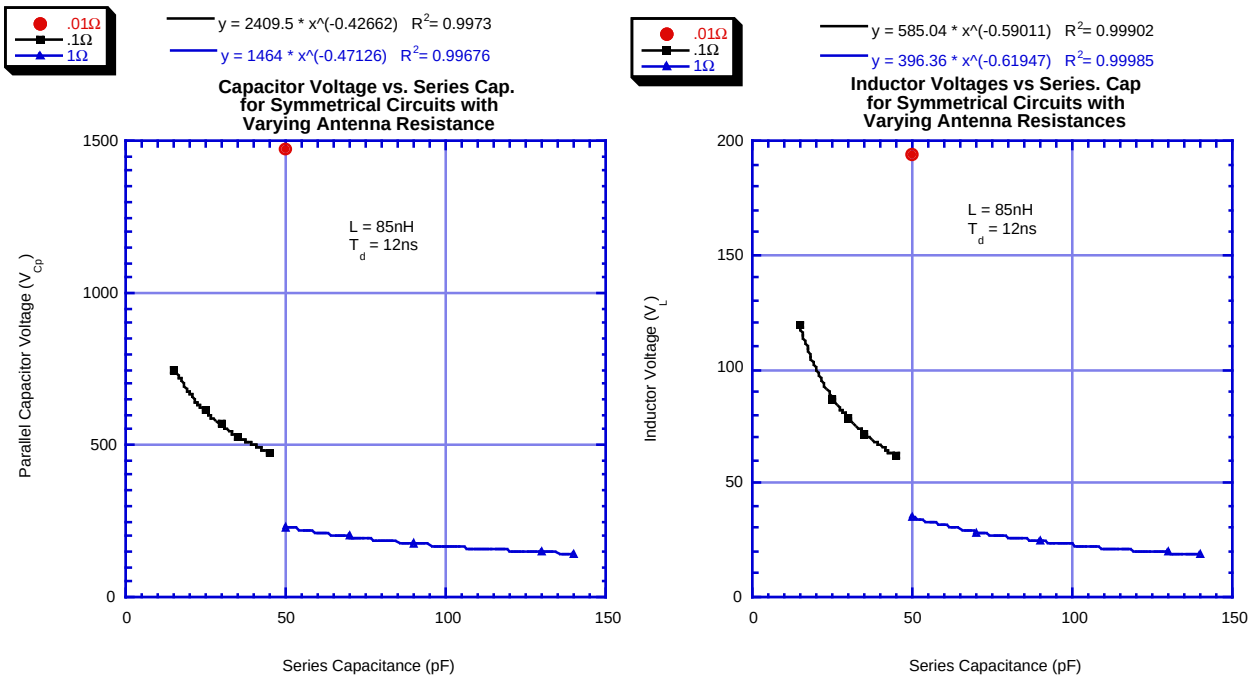

Figures 8 and 9. Plots of parallel capacitor voltages (Figure 8) and inductor voltages (Figure 9) vs. series capacitance for varying antenna resistances. The antenna current is fixed at 15.8 A. Compare with Figures 4 and 5.

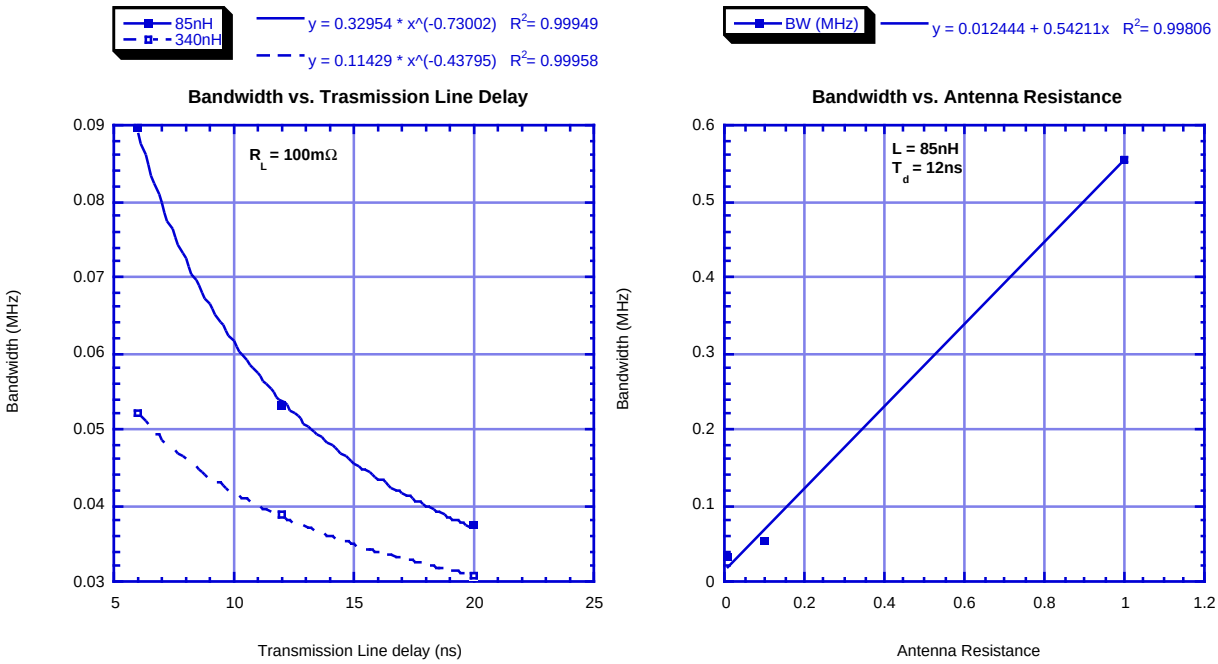

Figures 10 and 11. Bandwidth vs. transmission line delay (10) and antenna arm resistance (11). Q will vary linearly with inverse bandwidth. For an 85nH circuit with R = 100mΩ, Q will range between 100 and 300 over the 5-15 MHz frequency range.

III. Operating Curves: Asymmetric Variables

A. Antenna resistance

The resistance at L_1 (R_{L1}) was held at 100mΩ while the resistance at L_2 was set to 10mΩ and 1Ω, while maintaining symmetrical inductances of 85nH or 340nH (see Figures 6-9). Within this range, antenna arm currents remained nearly constant along the operating curves. However, the current values depend upon the total antenna resistance (i.e., the sum of the two antenna arm resistances). In the first case, a total antenna resistance of 110mΩ yielded currents of 21.3A in each antenna arm (the two antenna arm currents differed by less than 50mA), whereas a total antenna resistance of 1.1Ω yielded approximately 6.74A in each antenna arm (with a current difference of less than 185mA between the two antenna arms). This is compared to 15.8A in each antenna arm in a balanced circuit with 12ns delays and 85nH inductances. The comparatively small differences in antenna current due to asymmetric resistances can be explained by the fact that, at a given frequency, the antenna inductance and the inductance of the transmission line together supply a large fixed impedance when compared to the contribution from the antenna resistance. In the instance of balanced circuits with total antenna resistances of 200mΩ, operating curves have slopes of approximately 31. Operating curves (see Figure 10) for circuits with total antenna resistances less than 200mΩ will have steeper slopes, whereas curves for circuits with more than 200mΩ will have more gradual slopes. Given this information, approximate operating curves for circuits other than those explicitly simulated can extrapolated (i.e., it can be assumed that uniformly varying transmission line delays will have similar effects upon the operating curves as in the case of balanced circuits discussed above).

The plot of resonant frequency vs. series capacitance (see Figure 11) when the antenna arm resistances are 100mΩ (R_{L1}) and 10mΩ (R_{L2}) and inductances of 85nH will lie somewhat below that for the balanced circuit with 85nH inductances. Similarly to plots for balanced circuits, the curve for the unbalanced circuit with inductances of 340nH lies somewhat below that for the unbalanced circuit with inductances of 85nH. Curves for total resistances of 1.1Ω (R_{L1}=100mΩ, R_{L2}=1Ω) lie significantly "above" the balanced cases (once again the curve for 340nH lies somewhat below that for 85nH) and span a significantly wider range of series capacitance values (this can be seen in plots of operating curves as well). The dependence of operating curve slope upon antenna resistance can be exploited to compensate for unmodeled parasitic capacitances (e.g., the presence of a minimum value of series capacitance due to cabling, etc.) by the addition of resistors to the antenna arms.

Curves of parallel capacitor voltages for a given resistor configuration are roughly parallel, with the curves for 340nH lying slightly above the curves for 85nH. The curves for 110mΩ resistance are roughly parallel to those for 200mΩ (the balanced cases) as are those for 1.1Ω, though the latter have much lower offsets and, as mentioned above, span a larger range of series capacitance values. Curves of voltage across the parallel capacitor vs. series capacitance for 110mΩ lie slightly above those for 200mΩ and are roughly parallel to the former (though they span a smaller range of series capacitance values).

Asymmetry in resistance values leads to asymmetry in inductor voltages as well as phase differences between inductor voltages and currents (the phase differences between voltages and between currents are equal). Varying R_{L2} by a factor of ten in either direction while maintaining R_{L1} at 100mΩ

results in minimal phase differences and comparatively small voltage/current differences (current differences are noted on Fig. 6, phase and voltage differences on Figure 13). For curves where the inductances are 85nH, the phase difference between V_{L1} and V_{L2} (and, consequently, the currents as well) remains between 0.4˚ and 0˚ and for 340nH, the phase difference remains between –3˚ and 0˚. Inductor voltages may differ in magnitude by up to 3% in curves where the total resistance is 1.1Ω; otherwise, inductor voltages are equal to within less than 1%. Curves for 110mΩ lie only slightly above the corresponding baselines (85nH and 340nH), whereas curves for 1.1Ω lie significantly below the baselines and span a larger capacitance range.

B. Transmission Line Delay

To investigate possible effects of non-uniform transmission lines, circuits were simulated with one transmission line delay fixed at 12ns (the specification of the manufactured lines currently being used) while varying the second transmission line delay between 10ns and 14ns. Assuming identically constructed lines, this range would correspond to deviations of about ±1.5 feet in length.

Unlike the previous cases (asymmetry in resistance; symmetrically varying transmission line delay and/or inductances), inductor currents are not necessarily approximately equal along operating curves. However, *total* inductor current (that is, $I_{L1} + I_{L2}$) *is* constant. Furthermore, it is equivalent to the total inductor current for balanced circuits with 200mΩ antenna resistances (~31.6A total). The difference between antenna arm currents may be as high as ~2.2A and increases with increasing series capacitance. The operating curves for the two extreme cases are approximately parallel to the operating curve for a balanced 85nH, 200mΩ circuit, with the 10ns curve lying minimally above the baseline curve and the 14ns curve lying minimally below. The same applies to the plots of resonant frequency vs. series capacitance as well as those of parallel capacitor voltage and inductor voltage (due to significant asymmetry in inductor voltages, the average of the two inductor voltages was plotted).

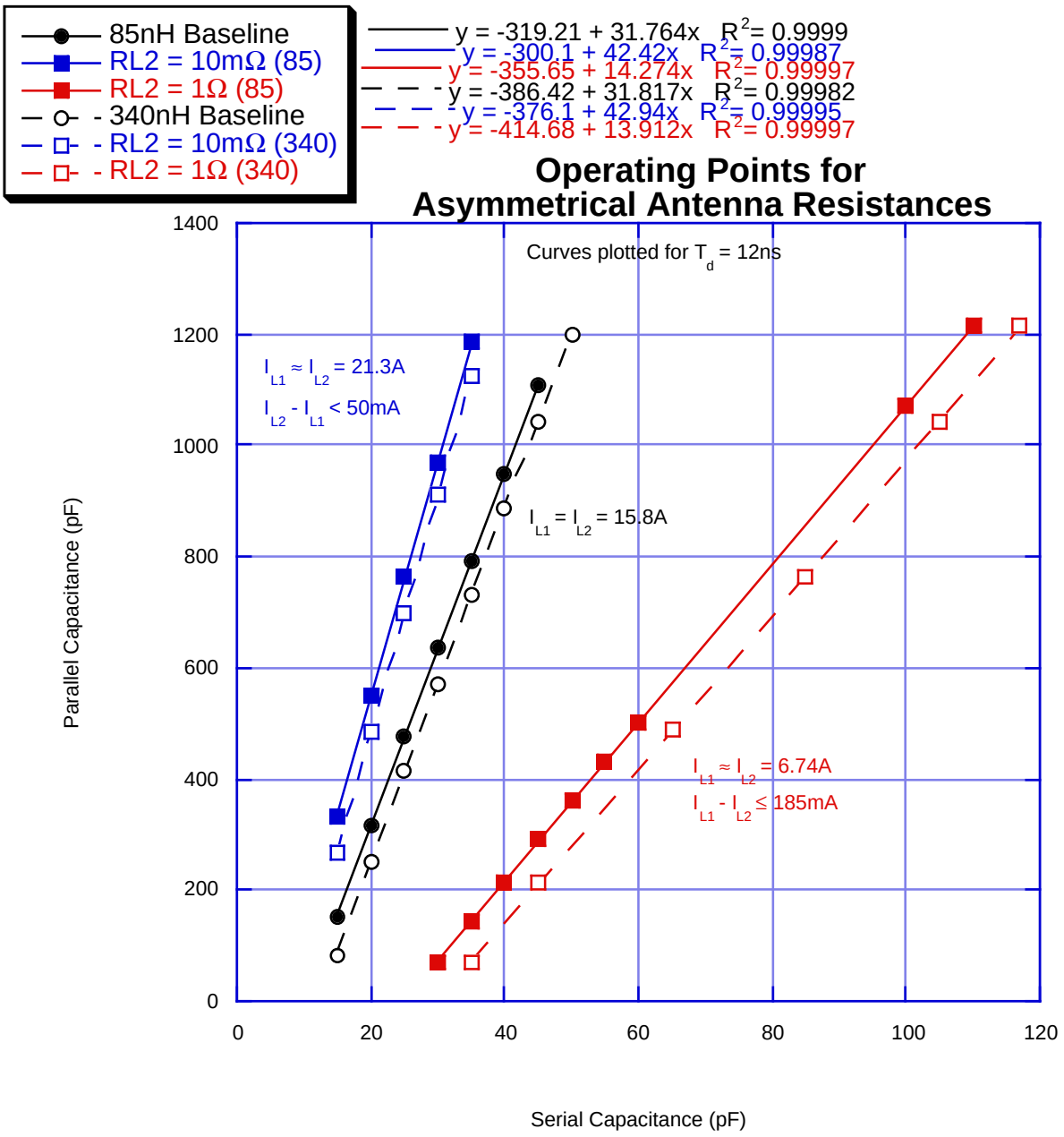

Figure 12. Operating curves for asymmetrical circuits with total resistances equal to 110mΩ and 1.1Ω at inductances of 85nH and 340nH. Operating curves for balanced circuits with total antenna-arm resistances of 200mΩ are shown for comparison. Curves of the same color and marker shape correspond to identical sets of antenna resistances. Filled curves represent circuits with inductances of 85nH and dashed curves represent 340nH circuits.

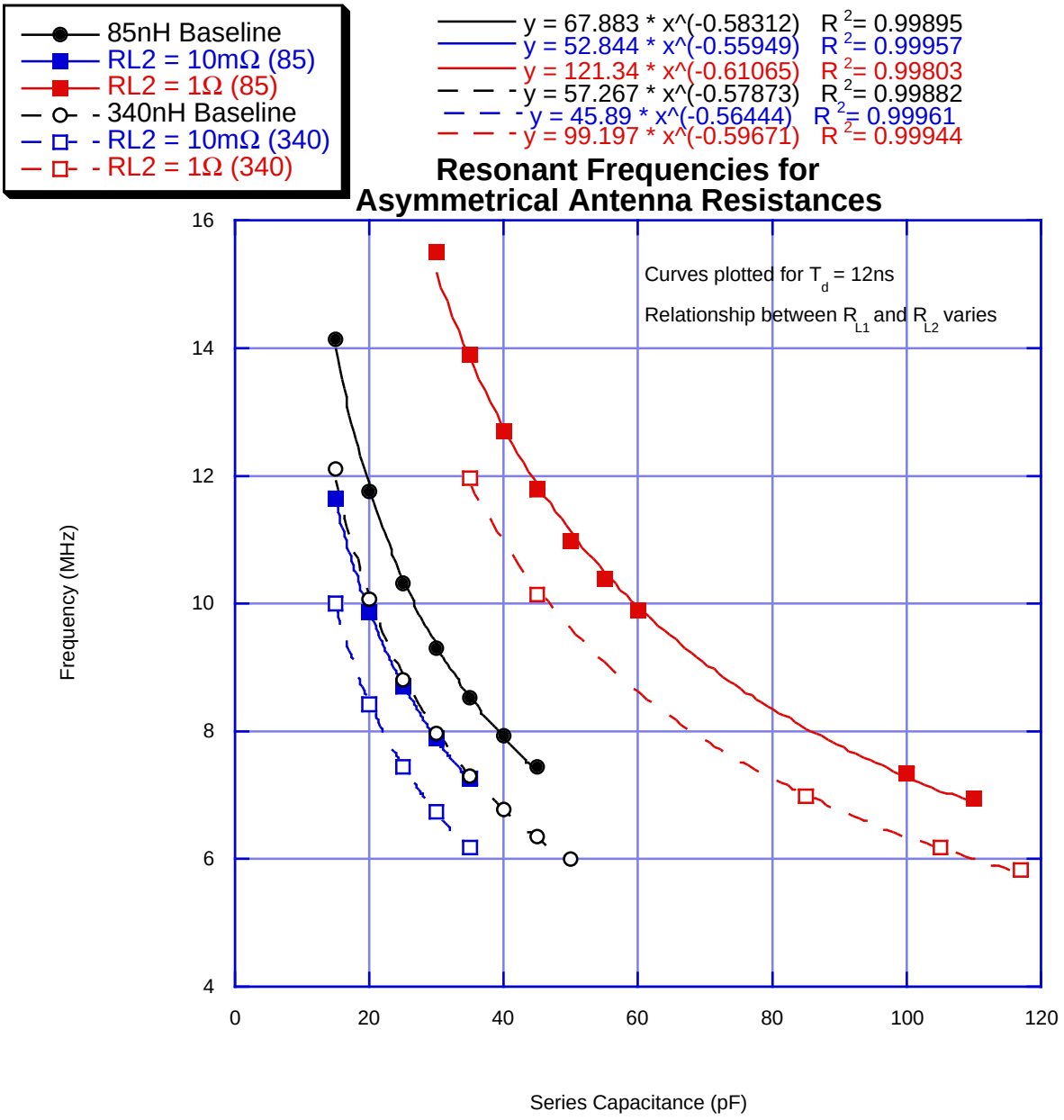

Figure 13. Resonant frequencies vs. series capacitance for asymmetrical circuits with total resistances equal to 110mΩ and 1.1Ω at inductances of 85nH and 340nH. Operating curves for balanced circuits with total antenna resistances (R_{L1}+R_{L2}) of 200mΩ are shown for comparison. Curves of the same color and marker shape correspond to identical sets of antenna resistances. Filled curves represent circuits with inductances of 85nH and dashed curves represent 340nH circuits

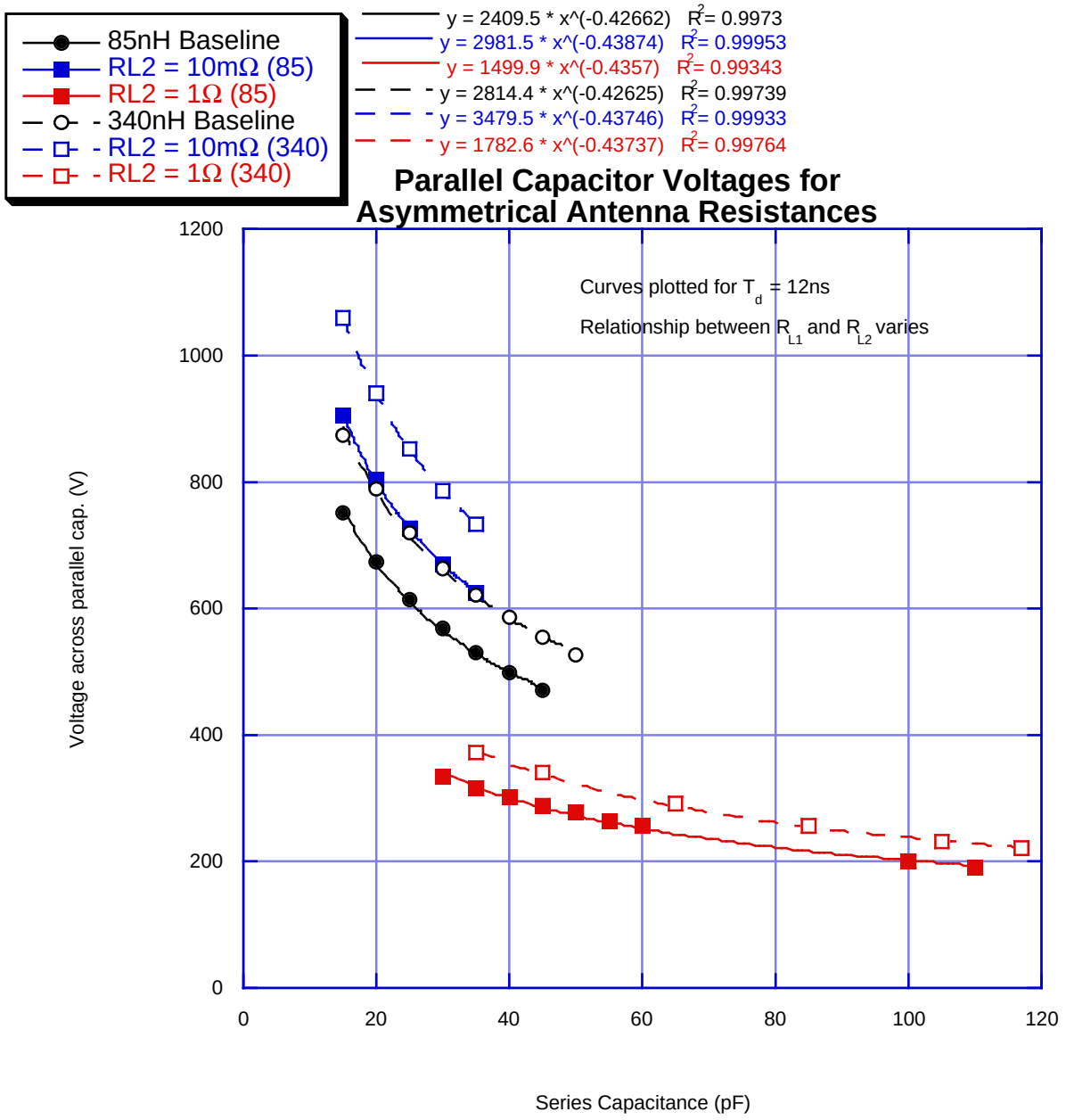

Figure 14. Parallel capacitor voltages vs. series capacitance for asymmetrical circuits with total resistances equal to 110mΩ and 1.1Ω at inductances of 85nH and 340nH. Operating curves for balanced circuits with total antenna-arm resistances of 200mΩ are shown for comparison. Curves of the same color and marker shape correspond to identical sets of antenna resistances. Filled curves represent circuits with inductances of 85nH and dashed curves represent 340nH circuits

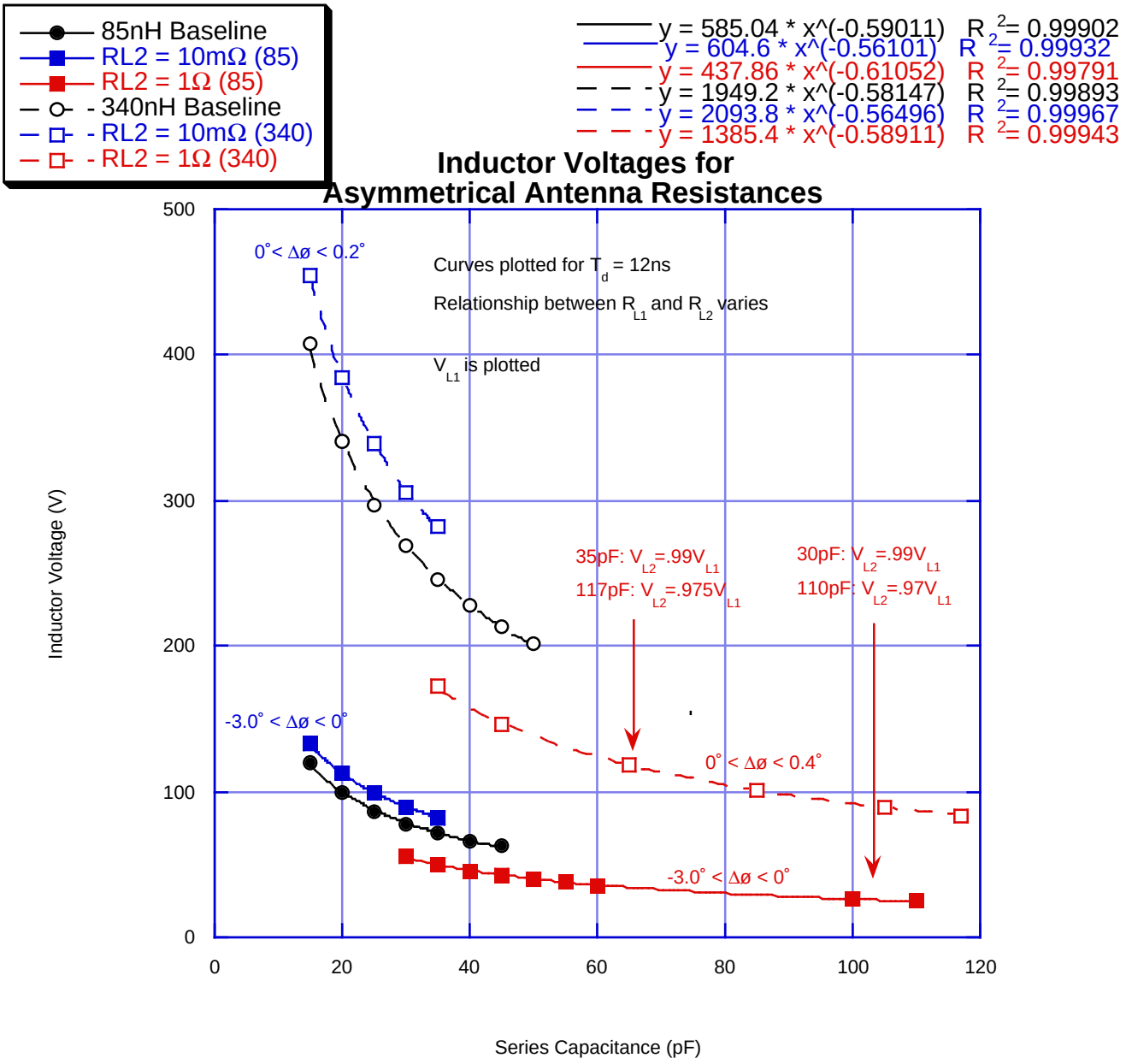

Figure 15. Inductor voltages vs. series capacitance for asymmetrical circuits with total resistances equal to 110mΩ and 1.1Ω at inductances of 85nH and 340nH. Operating curves for balanced circuits with total antenna-arm resistances of 200mΩ are shown for comparison. Curves of the same color and marker shape correspond to identical sets of antenna resistances. Filled curves represent circuits with inductances of 85nH and dashed curves represent 340nH circuits. Range of phase difference between V_{L1} and V_{L2} is noted alongside each curve where applicable. Information about relative values of V_{L1} and V_{L2} provided for 340nH curves. The difference in voltage on the two antenna arms is less than 1% for the 85nH curves.

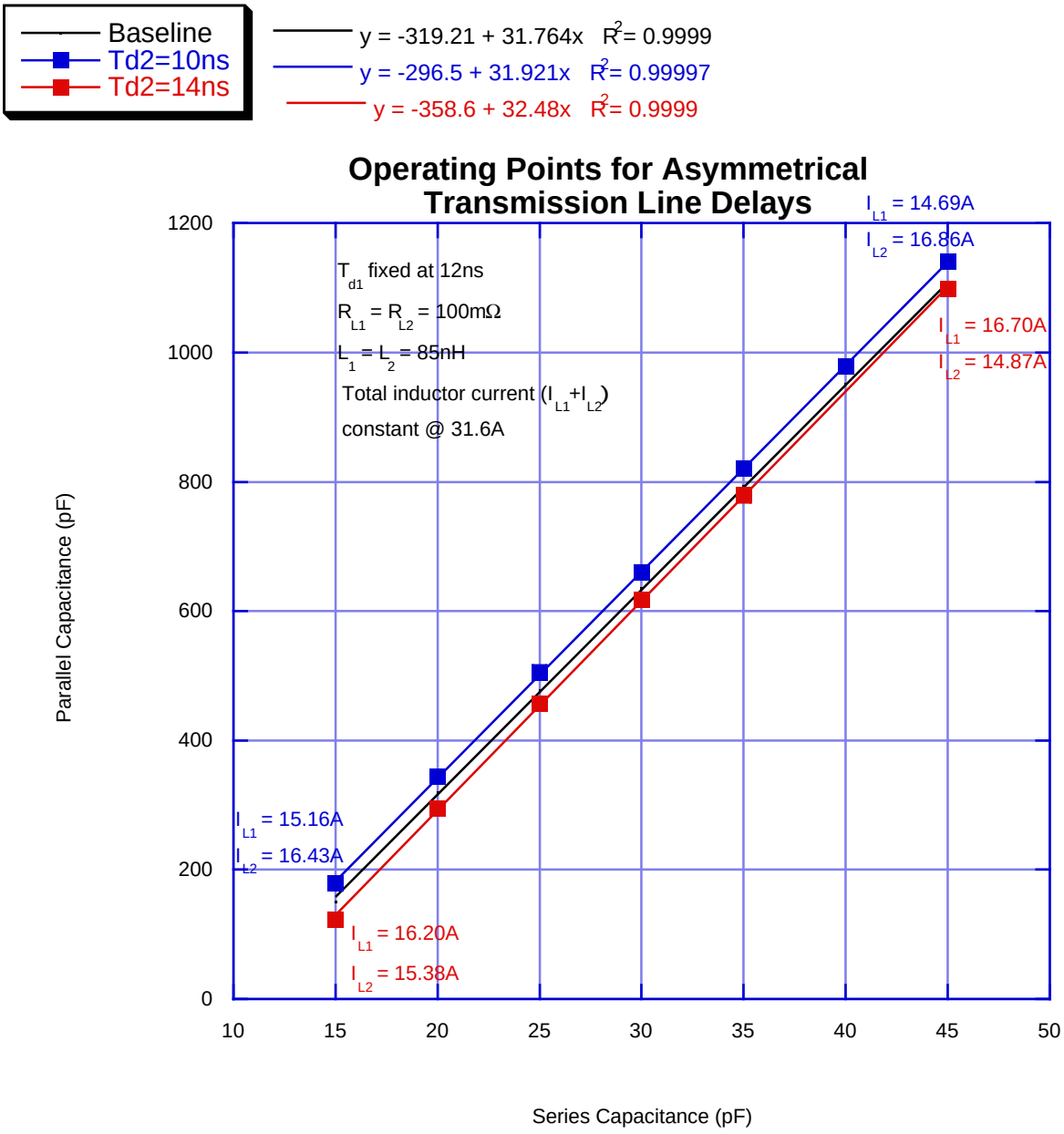

Figure 16. Operating curves for circuits with asymmetrical transmission line delays. Delay of the transmission line on L_1 was fixed at 12ns, while the second line was varied from 10ns to 14ns. Inductor currents are labeled at the endpoints of the two curves. Current imbalances increase with increasing series capacitance. The operating curve for a balanced (200mΩ) 85nH circuit is provided as the baseline.

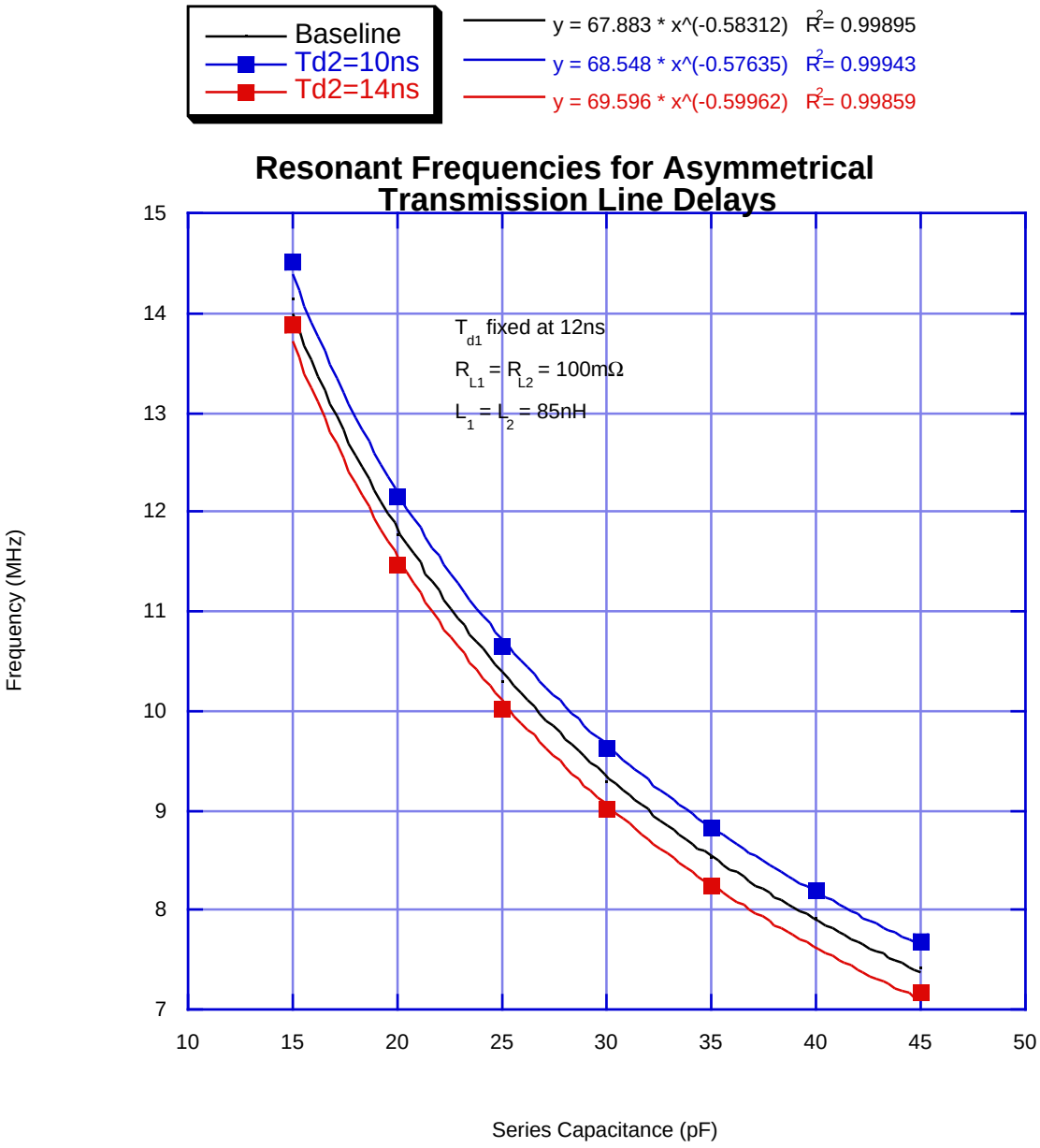

Figure 17. Resonant frequencies vs. series capacitance for circuits with asymmetrical transmission line delays.

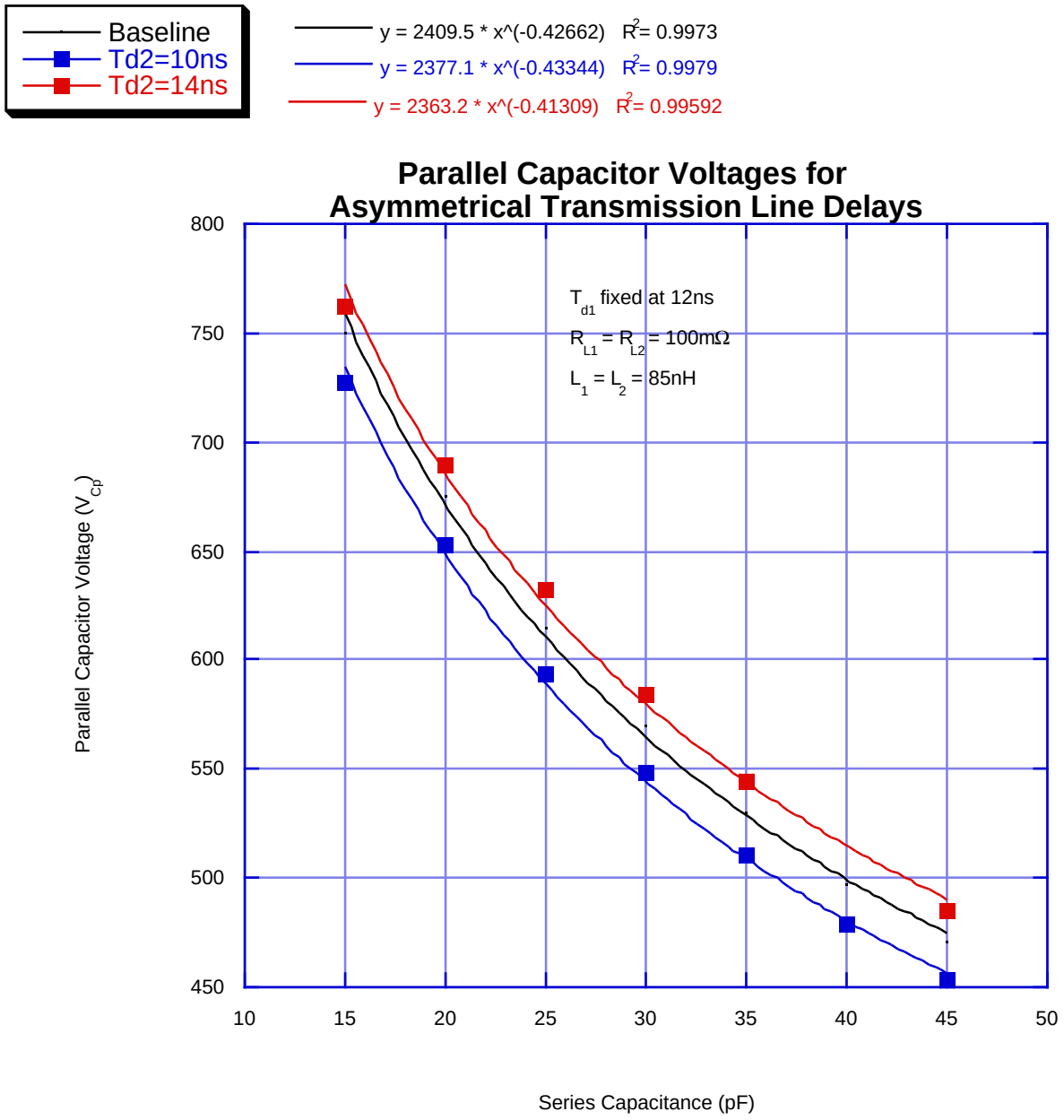

Figure 18. Parallel capacitor voltages vs. series capacitance for circuits with asymmetrical transmission line delays.

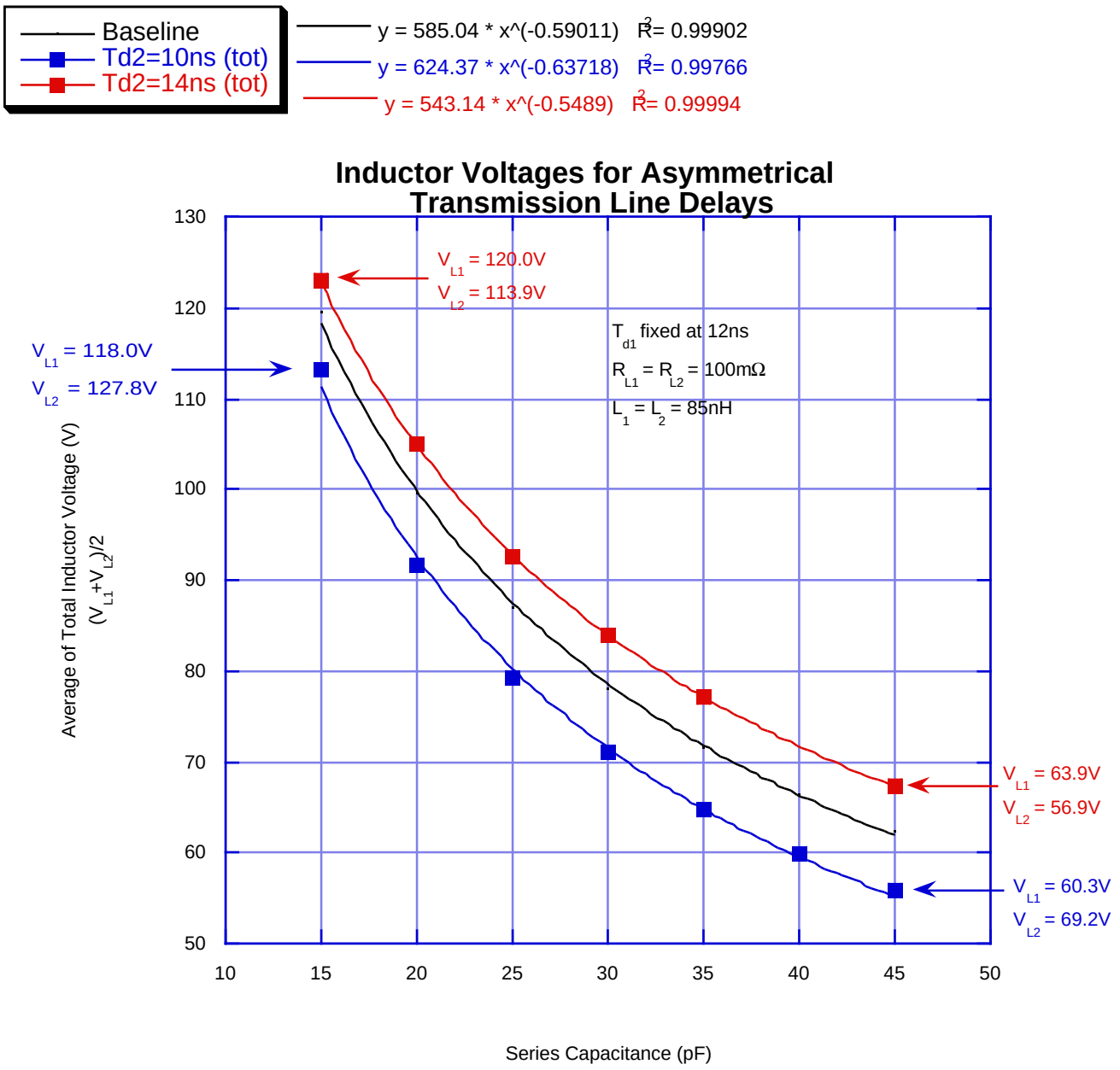

Figure 19. Inductor voltages vs. series capacitance for circuits with asymmetrical transmission line delays. Due to relatively large imbalances in inductor voltages, the average of the two voltages was plotted alongside the single-arm current from the balanced circuit.

IV. Summary

The simulations conducted confirm that the RMF_O/FRC antenna system can safely provide the 5G (peak) magnetic fields desired in the 5-15 MHz frequency range. The simulations suggest that the system will be relatively insensitive to asymmetries in its components and can operate over the 6-12 MHz range even if asymmetries are much worse than expected while still providing 5G fields which are roughly symmetrical between the two antenna pairs and between the two arms of each inductor. The simulations also suggest that desired operation can also be maintained in the presence of plasmas which have a large effect on the effective antenna resistance. For expected operating conditions, the circuit quality factor (Q) should range between 100 and 300 over the 5-15 MHz range in the absence of plasma, with circuit quality dropping by roughly a factor of 10 for plasmas which greatly increase the effective antenna resistance. For a given set of parameters, approximate operating points can be found with relative ease by extrapolating from the curves given above. Similarly, rough estimates of resonant frequency and circuit voltages can be made. In addition, simulated antenna currents depend only upon antenna resistance and can be found with minimal error (see equation in section II.C)

References

1. S.A. Cohen and R.D. Milroy, Physics of Plasmas **7**, 2539 (2000).
2. S.A. Cohen and A.H. Glasser, Physical Review Letters **85**, 5114 (2000).
3. A.H. Glasser and S.A. Cohen, Physics of Plasmas **9**, 2093 (2002).

Acknowledgements

Professor Samuel Cohen commissioned this report, determined its structure, suggested the simulations to be run, read several drafts, and made numerous corrections and additions. Dr. Ronald Hatcher provided guidance in the use of SIMmetrix, particularly concerning the modeling of transmission lines. Ethan Schartman provided an introduction to the RMF_O/FRC apparatus as well as assistance with creating circuit models in SIMmetrix. This report was made possible by the support of the Program in Plasma Science and Technology.